The Efficiency of Eco-friendly Corrosion Inhibitors in Protecting Steel Reinforcement

Amir Zomoridan, Regeane Bagonyi, Abir Al-Tabbaa

Department of Engineering, University of Cambridge, Cambridge CB2 1PZ, UK

Abstract

Reinforcing steel is used extensively in buildings to provide strength and integrity to the concrete structure. This material is, however, highly susceptible to corrosion in chloride-contaminated environments, which increases the risk of structural instability and failure. This work characterises the mechanisms and efficiency of corrosion protection offered by sodium nitrate, casein, and two amino acids (11–aminoundecanoic acid, and p–aminobenzoic acid) in simulated concrete pore solutions with different contents of chloride ions. The performance of each inhibitor in the critical chloride concentration (C_{cirt}) was investigated using electrochemical techniques. Open circuit potential and linear polarisation were used to identify the C_{crit} in synthetic pore solutions. Potentiodynamic polarisation and electrochemical impedance spectroscopy were performed to evaluate the corrosion activities and the passivation mechanism of inhibitors in C_{crit}. Results indicate that reinforcing steel can be protected through an appropriate selection of corrosion inhibitors. Among of the inhibitors studied here, casein demonstrated the highest corrosion inhibition efficiency with minimum current density of 9.19×10^{-8} μA/cm^2 and inhibitor efficiency of more than 80%. Casein provides passivity to the reinforcing steel in the presence of the C_{cirt} in the pore solution.

Key words: Inhibitor efficiency, Pore solution, Corrosion protection, Electrochemical tests

Introduction

The corrosion of reinforcing steel is a major cause of failure in concrete structures and has a detrimental effect on the sustainable use of natural resources and on the economy [1]. It has been estimated that the global cost of corrosion is US$2.5 trillion, equivalent to 3.4% of the global gross domestic product (GDP) of 2013, and this cost includes neither individual health and safety nor environmental consequences [2]. It is, therefore, important to develop technologies that promote corrosion protection and enhance the service life of concrete structures [3].

The concrete matrix itself provides initial physical and chemical protection to the embedded steel. This physical barrier retards the ingress of aggressive species such as chlorides, carbon dioxide, sulphates, oxygen and moisture and its high alkalinity also offers chemical protection through the formation of stable iron oxide on the surface of the reinforcement [4]. Generally, the corrosion mechanism of steel consists of anodic reactions, associated with the dissolution of iron ions from the steel, and cathodic reactions, or reduction processes (Reactions 1 and 2). Chemical reactions of species produced in anodic and cathodic processes initiate the formation of iron hydroxide (Reaction 3); this formation, in turn, tends to react further with oxygen to form higher oxides (Reaction 4) [5]. These iron oxides are stable at the high pH of the concrete according to the Pourbaix diagram [6].

$$Fe_{(s)} \leftrightarrow Fe^{2+} + 2e^{-} \quad \text{Reaction (1)}$$

$$H_2O + \frac{1}{2}O_2 + 2e^{-} \rightarrow 2OH^{-} \quad \text{Reaction (2)}$$

$$Fe^{2+} + 2OH^{-} \leftrightarrow Fe(OH)_2 \quad \text{Reaction (3)}$$

$$6Fe(OH)_2 + O_2 = 6H_2O + 2Fe_3O_4 \quad \text{Reaction (4)}$$

Initial physical and chemical protection can, however, be interrupted due to carbonation or ingress of chloride ions which are detrimental to the protective film. Failure in the protective, or passive, film

induces a new cycle of oxidation and reduction processes and causes further corrosion of the embedded steel.[7]. The subsequent formation of the expansive corrosion product on the surface of the reinforcement has been established as a cause of cracking and spalling of the concrete, which in turn creates easier paths for the aggressive ions to reach the reinforcement and thus, accelerates the corrosion and degradation process [8].

Many factors affect the degradation of passive film and two are particularly important: the concentration of chloride ions adjacent to the reinforcing steel, and the chloride binding capacity of the concrete matrix. The initial concentration of chloride ions required to break down the passive film we term C_{crit} [9,10]. The initial concentration of chloride ions needed to break down the passive film is dependent on the alkalinity of the concrete, and therefore the concentration of the chloride ions in the vicinity of the rebar surface is commonly expressed by $[Cl^-]/[OH^-]$[11,12]. There is, however, uncertainty about C_{crit} because the ingress of chloride ions into the concrete matrix is affected by the binding, chemically or physically, of chloride to the hydration products which decreases the tendency of chloride to react with the iron oxide. Various studies have demonstrated a positive effect of additives such as silica fume and fly ash in increasing the critical level of chloride ions (C_{cirt}) due to binding with chloride ions and subsequently hindering the initiation of the corrosion process[11,13].

Adding corrosion inhibitors to the concrete mixture can thus increase the C_{cirt} which subsequently increases the durability of the concrete structure in chloride contaminated areas. The mechanism of corrosion protection of such inhibitors is varied, and is dependent on the nature of the inhibitors. The main mechanism is based on impeding the cathodic and anodic reactions on the surface of the steel. The majority of inorganic inhibitors such as sodium nitrites and monofluorophosphates impede the anodic reactions, inhibiting corrosion in reinforced concrete, and are widely used in large construction projects and buildings. However, they have proven to be toxic to humans and their use in Europe is being questioned[14,15]. An alternative is to use organic inhibitors such as amino-alcohols, which, due to their high vapour pressure, can penetrate through the concrete and react with the surface of the reinforcing steel [16,17]. The mechanism of corrosion inhibition is based on surface adsorption of the inhibitors on the steel, which blocks other aggressive ions from reacting with the steel [18]. The development of hybrid corrosion inhibitors, being mixes of different types of inhibitors, has improved effectiveness further. For instance, *Pan et al*. synthesized imidazoline which comprises a symmetrical molecular structure with two imidazoline heterocycles and two alkyl long chains of lauric acid [19]. However, complex, expensive procedures are not ideal and highlight the need for a new approach to find affordable, efficient inhibitors with low environmental toxicity.

Recently, therefore, attention has been given to the development of natural and environmentally friendly corrosion inhibitors. Casein, which is best known as a protein in dairy milk, contains multi-functional groups that are able to initiate intermolecular reactions and adsorb spontaneously onto the stainless steel surface [20]. The adsorption mechanism was reported to be slightly endothermic due to the energy required to break the intermolecular bonds of proteins and form a new bond at the protein/metal interface [21]. In addition, the molecular structure of the casein induces a noticeable super-plasticizing effect on concrete [22]. 11-aminoundecanoic acid, p–aminobenzoic and sodium nitrate are all produced artificially for the food industry or from natural origins and consist of many functional groups and have the potential to be used as green corrosion inhibitors. There is, however, little information about the efficiency of any of these greener materials to protect reinforcing steel against the corrosion in pore solution. The aim of this research is, therefore, first to establish the critical concentration of chloride ions at which corrosion of reinforcing steel is initiated (C_{crit}), and then to evaluate the performance and efficiency of green inhibitors in pore solution at C_{crit}.

Materials and methods

Commercial reinforcing steel was obtained from a local supplier and then sectioned into plates with diameters and thicknesses of 10 mm and 3 mm, respectively. The chemical composition of the rebar is presented in Table 1.

Table 1: Chemical composition of the reinforcing steel

Chemical composition (%wt)	C	Mn	Si	S	Cr	Ni	Cu	Fe
Reinforcing steel	0.19	0.82	0.13	0.02	0.1	0.14	0.57	Balance

All electrochemical tests were performed in a pore solution containing 0.1M NaOH, 0.3M KOH and saturated with $Ca(OH)_2$. This solution has a similar chemical composition to a pore solution extracted from cement paste samples with w/c=0.42, wet cured for 7 days as described elsewhere [23]. Four corrosion inhibitors were tested: sodium nitrate (0.05M), casein (9.7×10^{-4}M), 11–aminoundecanoic acid (0.05M), and p–aminobenzoic acid (0.05M). The details of evaluated systems are described in Table 2. The 11–aminoundecanoic acid and p–aminobenzoic acid will henceforth be referred to as 11-AD and 4-AB, respectively.

Table 2: Details of the chemical composition of the testing solution used to evaluate the corrosion activity in reinforcing steel

	Pore solution			Chloride	Corrosion Inhibitor			
System tested	NaOH (mol/L)	KOH (mol/L)	Ca(OH)2 (mol/L)	[Cl]/[OH]	Sodium nitrate(mol/L)	Casein (mol/L)	11-AD (mol/L)	4-AB (mol/L)
1	0.1	0.3	saturated	0, 0.4, 0.8, 1.2, 1.6, 2, 3	0	0	0	0
2	0.1	0.3	saturated	2	0.05	0	0	0
3	0.1	0.3	saturated	2	0	9.7×10^{-4}	0	0
4	0.1	0.3	saturated	2	0	0	0.05	0
5	0.1	0.3	saturated	2	0	0	0	0.05

Electrochemical studies of reinforcing steel in synthetic pore solution

In order to evaluate the corrosion activities of reinforcing steel, electrochemical tests were performed in a 100ml corrosion cell using a potentiostat PGSTAT 204 AUTOLAB. A three-electrode electrochemical cell consisted of a platinum plate as a counter electrode, an Ag/AgCl reference electrode and rebar with the surface of 1 cm^2 as the working electrode. The potential of reinforcing steel (OCP) or half-cell potential allows characterization of the metal/electrolyte interface in a rapid and non-destructive way. The OCP represents the variation of potential with time and these values are sensitive to the change of surface condition, composition, and pH of the solution. This potential was monitored with respect to the silver chloride reference electrode for 24 hours before performing linear polarization to ensure that the change in potential with time (dV/dt) is less than ≤ 1 μV/s for two continuous hours. Evaluation of the steady state potential of the working electrode and all electrochemical studies were undertaken at room temperature (23 ± 2 °C).

Linear polarization with a sweep of ± 20 mV from the OCP and scan rate of 1 $mV.s^{-1}$ was performed.

In order to obtain the corrosion current density (i_{corr}), polarization resistance, R_p, which is defined as a slope of a potential-versus-current density line within the zero current point $i = 0$, equation 1 was used for calculating above mentioned parameters [24,25]. Additionally, the Stern–Geary constant (Eq. 2), which is calculated from the anodic and cathodic Tafel slopes, b_a and b_c, respectively, was used to obtain the corrosion current density.

$$R_p = \left(\frac{\partial \Delta E}{\partial i}\right) \qquad \text{Equation (1)}$$

$$B = \frac{b_a.b_c}{2.303(b_c+b_a)}$$ Equation (2)

Once the Rp and B are defined, the corrosion current density can be calculated using Eq. 3.

$$i_{corr} = \frac{B}{R_p}$$ Equation (3)

Corrosion potential (E_{corr}) can be identified from the Tafel plot when the anodic reaction rate is equal to the cathodic reaction rate and there is no net current flow. The electrochemical parameters associated with the polarization measurements such as corrosion potential (E_{corr}), corrosion current density (i_{corr}), Tafel slopes (b_a, b_c) and corrosion rate (CR) were obtained using AUTOLAB software. A Potentiodynamic polarization test was carried out by applying a range of potential -300 mV to +1.1V versus reference electrode with a sweep rate of 0.1 mVs^{-1}

The efficiency of each inhibitor in preventing corrosion is expressed as a percentage (%IE), calculated using Eq (4).

$$\%IE = \frac{io-i}{i} \times 100$$ Equation (4)

where i and i_0 represent corrosion current density without and with the use of inhibitors.

Three replicates were used for each experiment under the same conditions and the average results were reported.

Electrochemical Impedance Spectroscopy (EIS)

To better understand the mechanisms of inhibition involved, Electrochemical Impedance Spectroscopy (EIS) was also periodically used. Data collection was performed at the open circuit potential, during immersion in the synthetic pore solution (pH 13.2) at room temperature. A signal of 10 mV rms was imposed and the frequency ranged from 100 kHz down to 10 mHz, using an AUTOLAB PGSTAT204. A three-electrode electrochemical cell was used inside a Faraday cage with the cell set-up as described earlier and the data was modelled with the appropriate equivalent circuit using Zview software.

Results and discussion

1.Half-cell potential

In order to determine the chloride threshold of the reinforcing steel in synthetic pore solution, the variation of the potential in different chloride concentration monitored for 24 hours. The results are presented in Figure 1.

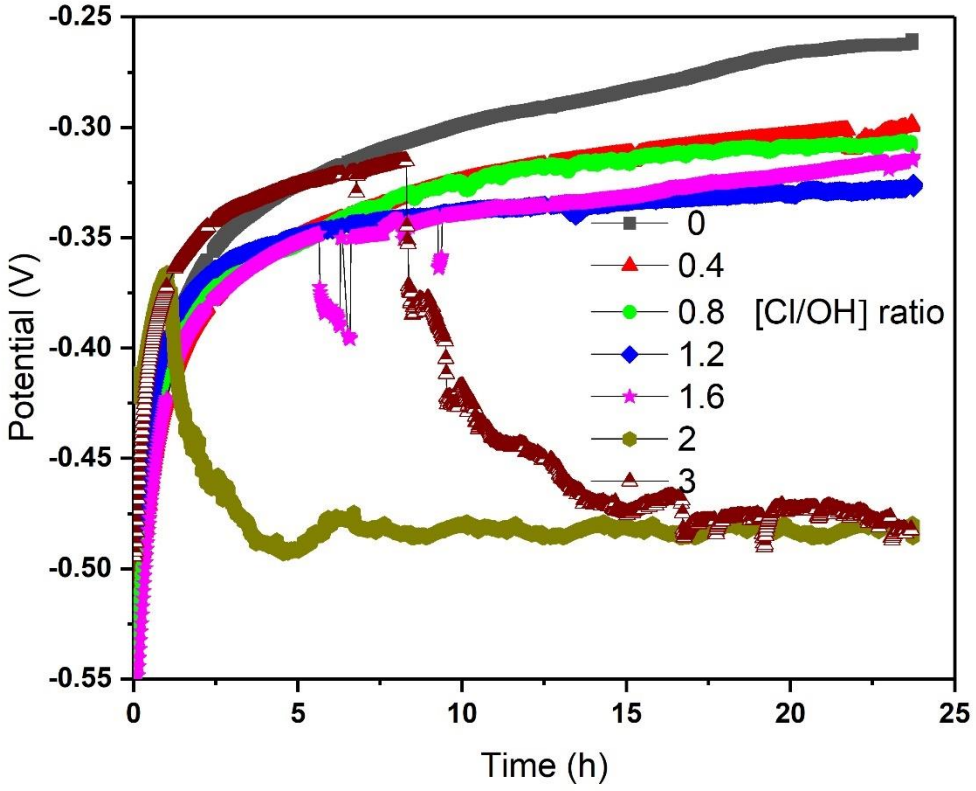

Figure 1: Variation of OCP value for reinforcing steel in synthetic pore solution at different ratios of [Cl]/[OH] in absence of corrosion inhibitor.

The initial value of the OCP in the non-chloride solution was in the region of -0.55 V and it gradually shifted to a more positive potential. The increase in potential was expected and was due to the formation of the passive oxide film on the reinforcing steel. The protective hydroxide $Fe(OH)_2$ or stable iron oxide, according to the thermodynamic diagram of Pourbaix and Reaction 3, is formed in the alkaline synthetic pore solution [6]. This passive film is composed of a double layered structure: an inner layer rich in Fe^{2+} and an outer layer rich in Fe^{3+} hydroxides [26]. Other investigations show that passive film can be formed in two stages: the first stage, which takes place within hours is related to the formation of a dense and compact Fe II oxide layer, while the second stage is related to the thickening of the film [27,28]. The increase of OCP over time was a result of the formation and growth of the protective passive layer on the reinforcing steel. The growth rate of the protective layer was, however, limited and the OCP reached a plateau after 20 hours of immersion. There is some evidence to suggest that the thickness of the passive oxide film is typically in the range of 3 to 15 nm and it was affected by the composition of the solution [27]. For instance, saturated calcium hydroxide in solution forms a $Ca(OH)_2$-rich layer on the steel and hinders the cathodic reactions [29,30]. The final OCP value after the formation of the protective passive layer was approximately -0.25 V. This value was consistent with the OCP value obtained in the simulated concrete pore solution reported in the literature [14].

1.1 Effect of chloride ions

The addition of chlorides to the synthetic pore solution had a detrimental effect on the OCP and caused a smooth shift of the OCP to the cathodic potential. Studies show that the chlorides alter the passive film stoichiometry by increasing the ratio of Fe^{3+} to Fe^{2+} in the metal–film interface [31]. The mechanism describing the impact of the chlorides on the passive film has been investigated by Dormohammadi et al. Based on this mechanism, de-passivation of the reinforcing steel has multiple stages: in the first stage chloride ions initiate interaction with the high energy iron ions in the passive film. Due to the high concentration of OH^- in the solution, chloride ions cannot form a stable bond with iron ions and the chloride ions in newly formed iron chloride were immediately replaced with hydroxide

and formed $Fe(OH)_3$ [31]. Absorption of three OH^- ions from solution decreases the local pH at the interface of the electrolyte and passive film. In the next stage, chloride ions slightly dragged out the iron ions from the passive film. Lowering the concentration of OH^- at the interface promotes formation of the $Fe(OH)_2Cl$ which is not soluble in the solution. The continuous attack of the chloride ions as described above caused formation of $Fe(OH)Cl_2$ or $FeCl_3$ on the surface which are soluble in the electrolyte. The $FeCl_3$ and $Fe(OH)\ Cl_2$ are converted to $Fe(OH)_3$ in the electrolyte releasing the chloride ions to the electrolyte where they can participate in another catalytic cycle of de-passivation [31].
The relation between the chloride concentration and open circuit potential is indicated in Figure 1. The smooth shift of potential to the negative value can be related to the decrease of the passive film thickness and initial interaction of chloride ions and iron ions in the passive film structure as described earlier. De-passivation of the reinforcing steel needs a sufficient number of chloride ions to decrease the local pH and form enough soluble $FeCl_3$ and $Fe(OH)_2Cl$ to break down the passive film in the reinforcing steel. The critical concentration of chloride ions for de-passivation was achieved when the ratio of [Cl]/[OH] reached 2 and, subsequently, a significant breakdown in potential was observed, clearly indicating the pitting initiation and de-passivation in the reinforcing steel. The corrosion potential in this critical concentration reached the value of -0.48 V and showed small fluctuations within a range of 0.03 V of this potential.

1.2 Effect of inhibitors

The addition of inhibitors to the pore solution containing the critical concentration of chloride ions strongly influences the OCP values as shown in Figure 2.

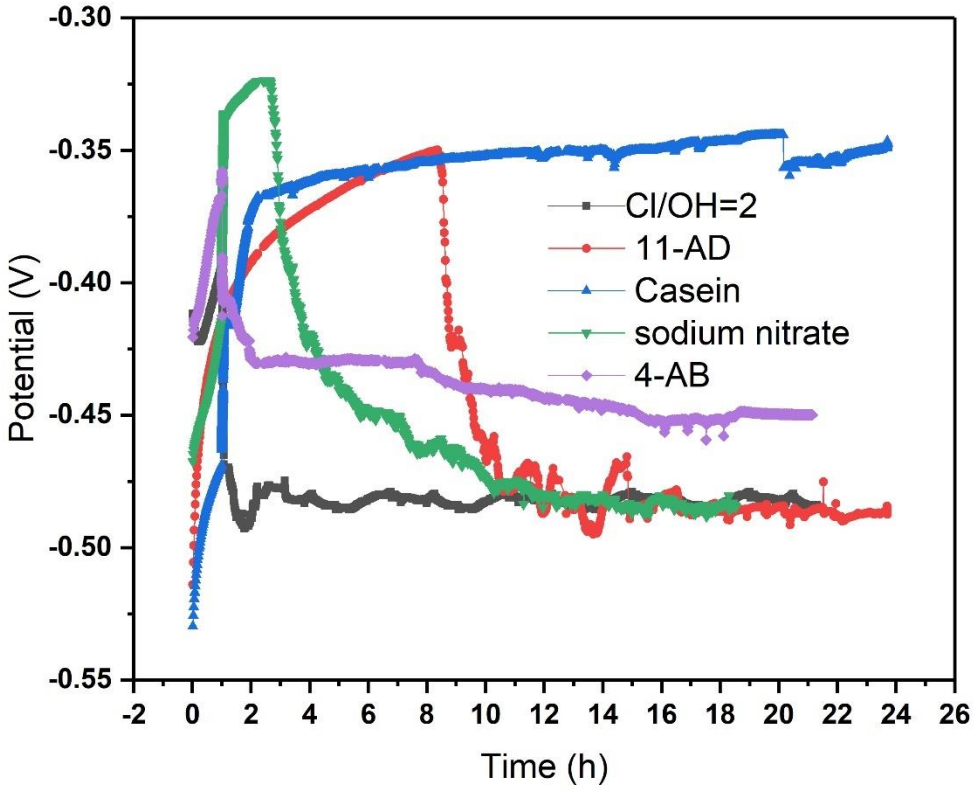

Figure 2: The OCP value of reinforcing steel in synthetic pore solution with different inhibitors at critical concentration of Cl/OH ratio

According to the ASTM C876-09, the active corrosion of embedded rebar in cement is identified when the OCP value is more negative than -0.273 V. However, environmental parameters such as availability

of oxygen as described earlier, Reaction 3, or of other additives, influence the corrosion process and OCP values [32]. In this research, sodium nitrate, as an inhibitor, shifted the potential of the reinforcing steel (-0.48V) to a more positive value. Nitrates are considered to be anodic inhibitors that form an insoluble protective film on the anodic spot of the corroding steel and block further anodic reaction and subsequently the surface of the steel is re-passivated [24]. The increase of OCP in the presence of sodium nitrate was limited to the first few hours and a subsequent breakdown in OCP was observed and the potential shifted to the cathodic values close to the potential of corroding steel (-0.48V). Breakdown in potential can be linked to the pH and availability of oxygen in pore solution since nitrates can enhance formation of passive film in acidic solution. Indeed, the passive film is nearly independent of nitrates in the alkaline solution [33,34].

The application of 11AD, the second inhibitor, promoted a limited sustained shift to positive potential for only 8 hours; it then exhibited a breakdown toward the corroding potential. Similarly, when 4AB was used as an inhibitor the OCP broke down, but nevertheless after this collapse the recorded OCP value was -0.42 V, which was still higher than the corroding potential of the reinforcing steel (-0.48 V) as shown in Figure 1. Although this potential is more anodic (more positive) than the corroding potential, there is still a high risk of corrosion according to the ASTM standard C876-91.

In contrast, casein shifted the OCP of the corroding steel to the noble values and no significant decrease or breakdown in OCP was observed during immersion in pore solution containing C_{cirt}. The enhanced passivity of reinforcing steel even at C_{cirt} can be attributed to the absorption of casein into the surface of the steel since casein contains many polar functional groups such as carbonyl, amide and amino groups [35]. The availability of these polar groups may facilitate formation of a complex of iron oxide and casein on the surface and subsequently change the chemistry of the interface. The OCP value of the passivated reinforcing steel in the presence of casein was approximately -0.32 V, which is 0.280 V higher than the corroding OCP potential.

2. Electrochemical analysis

2.1 Linear polarisation resistance

2.1.1 Effect of chloride ions

The polarisation resistance (Rp) of the reinforcing steel as a function of the chloride concentration is shown in Figure 3. Polarization resistance is defined as a slope of the current versus potential in a range of ±20 mV from the OCP value. This range was selected because limited sweeping potential and small scan rate guarantee enough acquisition data points to identify the slope with the minimum disturbed potential for the irreversible reactions in the reinforcing steel [36].

Results show that the polarisation resistance decreased with increasing chloride concentration. However, a sharp decrease of the polarization resistance was observed when [Cl]/[OH] =2 and it was assigned as the critical concentration of chloride (C_{crit}). The decrease the polarisation resistance before C_{crit} could be related to the formation of defects in, or decreasing thickness of, the passive film. This sharp decrease is also a clear sign of de-passivation of the reinforcing steel in synthetic pore solution.

The corrosion current density (i_{corr}) of reinforcing steel in different pore solutions was calculated using Eq. (3) where Rp was obtained from linear polarisation tests and B was extracted from the Tafel plot [37]. It has been reported that the B value is equal to 26 and 52 mV for the active and passive states of the steel, respectively. These values are widely used in estimations of the corrosion rate of reinforcing steel [37,38]. The value of B depends on many parameters: the conductivity of the electrolyte and ion transport, which participate in redox reactions (in concrete), the pH of the electrolyte and the type of passive film on the surface of the reinforcing steel. Thus various values have been reported for the constant B value [37,39,40]. In this study, the value of B was calculated using anodic and cathodic branches of the Tafel slope to identify the corrosion current density in the Stern–Geary formula. The results are shown in Table 3.

Table 3: Variation of corrosion current density and its correlation with chloride concentration using the Stern–Geary formula

[Cl]/[OH]	i_{corr} (µA/cm^2)	E_{corr} (V)	B(V)	b_a (V/decade)	b_c (V/decade)
0	0.06	-0.267	0.029	0.214	0.101
0.4	0.13	-0.306	0.036	0.253	0.128
0.8	0.20	-0.310	0.037	0.265	0.128
1.2	0.12	-0.331	0.038	0.310	0.122
1.6	0.13	-0.330	0.033	0.218	0.116
2	1.2	0.492	0.023	.089	0.141

As shown in Table 3, the highest current density is 1.2 µA/cm^2 when [Cl]/[OH]=2 which can be considered the critical chloride concentration; the corrosion current density (i_{corr}) of the steel did not significantly change in the pore solution until the chloride concentration reached the critical value.

Although the value of B from the Stern–Geary formula was calculated by measuring the Tafel slope, the R_p was obtained from the slope of current versus potential. Therefore, the polarisation resistance is independent of the B value and can be considered as an independent parameter in evaluating corrosion.

The average value of R_p diminished with the shift of the corrosion potential to cathodic values and with increasing concentration of the sodium chloride solution, as shown in Figure 3. Eventually polarisation resistance dropped to the value of 19kΩ when the chloride concentration reached the value of C_{cirt} and caused high significant rate of corrosion. Studies show that the critical concentration of chloride can change with the pH value of the concrete pore solution. For instance, in the synthetic pore solution with lower pH, C_{crit} is only 0.6 for de-passivation of reinforcing steel which is much lower than the value obtained in this research [12].

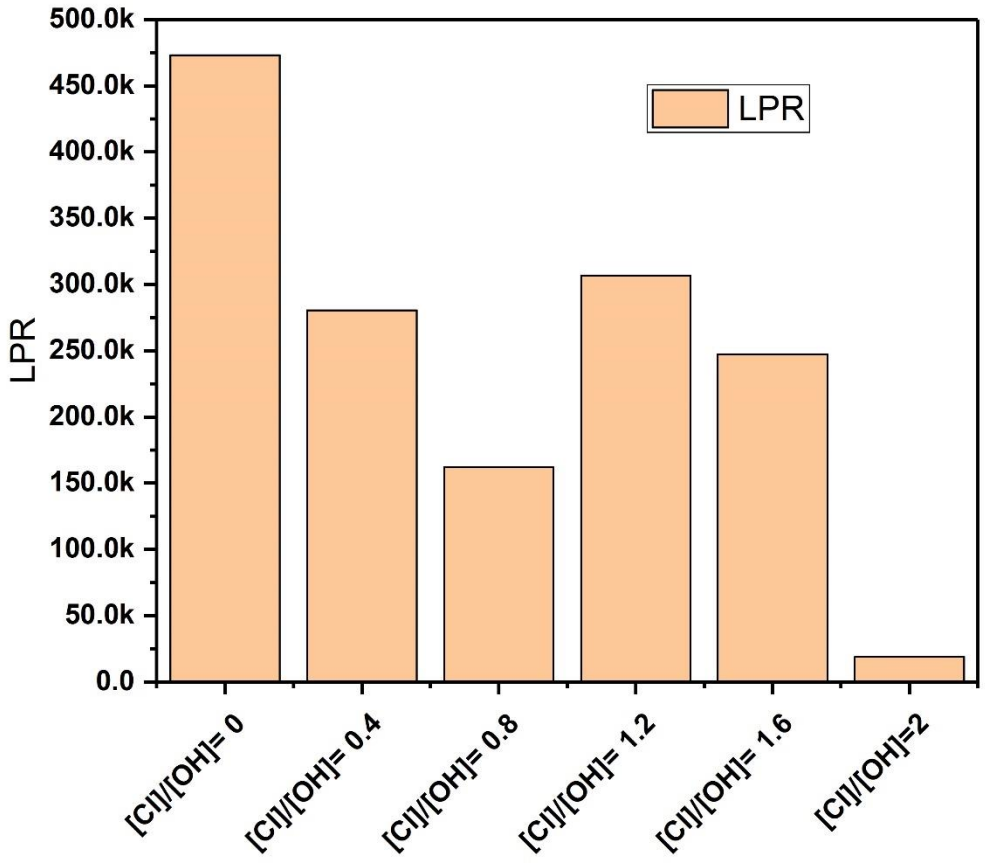

Figure 3: Polarisation resistance of the reinforcing steel in pore solution containing different chloride concentrations without the presence of corrosion inhibitors

Polarization results show that reinforcing steel is protected at lower concentrations than the C_{cirt} and addition of corrosion inhibitors had negligible effect on corrosion current density and polarisation

resistance of reinforcing steel (not shown here); therefore, further investigations were performed at critical chloride concentration (C_{crit}).

2.2 Potentiodynamic polarisation

2.2.1 Corrosion inhibitors

To corroborate the OCP results with another electrochemical technique, potentiodynamic studies were performed in pore solutions with and without inhibitor at [Cl]/[OH] = 2. All the tests were performed after 24h of immersion in the pore solution and the results are shown in Figure 4.

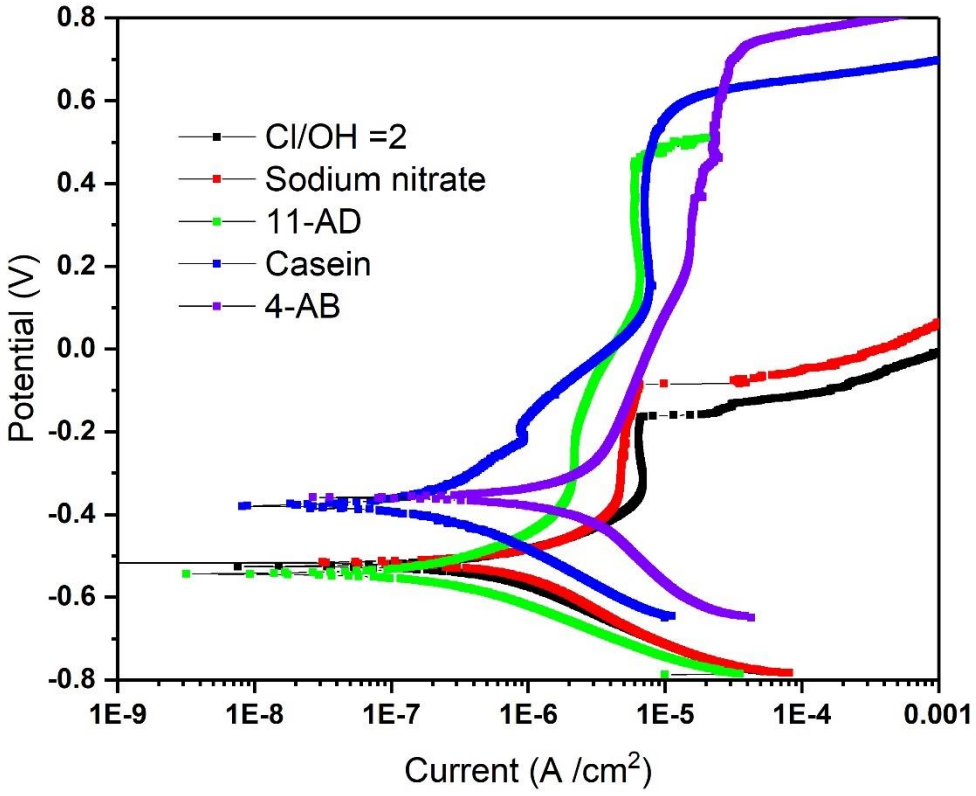

Figure 4: Potentiodynamic polarisation of the reinforcing steel in pore solution contains different types of inhibitor

The potentiodynamic results provide critical information about the corrosion potential, passivity of reinforcing steel and breakdown potential of the passive film when inhibitors participate in the corrosion process. The potentiodynamic polarisation of the reinforcing steel without inhibitors showed that the passive layer on reinforcing steel was formed in a limited range of potential, from -0.350V to -0.140V as seen in Figure 4. High alkalinity of the pore solution is the main reason for the formation of a passive layer, even at high chloride concentrations. However, due to chloride attack, this passive layer broke down at E_{pit}=-0.140V, which was much lower when compared to the pore solution containing inhibitors.

The current density of the passive film is constant regardless of the type of solution. Presence of the inhibitors in the pore solution may prolong the stability and consistency of the passive film. 11-AD significantly decreased the anodic current density before the formation of the passive layer, but the cathodic current and corrosion potential remained unchanged. The mechanism of 11-AD inhibition is based on blocking the anodic reactions and, subsequently, lowering of the current density during anodic scan [24]. 11-AD provided a stable passive layer with high breaking potential E_{pit}= 0.480 V, which is significantly higher than the pitting potential of reinforcing steel without inhibitors (E_{pit}= -0.140 V).

Sodium nitrate in pore solution did not protect the reinforcing steel significantly and corrosion current density and corrosion potential remained unchanged in comparison with the reinforcing steel in pore solution without inhibitors (Table 4). Table 4 presents the main kinetic parameters, the corrosion current density, Tafel slope and B for an apparent surface area of 1 cm^2 in presence of different inhibitors . the pitting potentials of reinforcing steel in the presence of sodium nitrate become slightly enhanced and reached the value of E_{pit}=-0.080V. It has been reported that nitrate ions compete with Cl ions in pore solution to form iron nitrate ($Fe[NO_3]_2$) instead of iron chloride ($FeCl_2$) and formation of iron nitrate on the reinforcing steel promotes formation a durable passive film [33,34,41]. However, high chloride concentration and the pH of the solution are critical parameters that may alter the protection performance of the sodium nitrate. H.Y. Ma *et al* used sodium nitrate in the acidic chloride solution and demonstrated that nitrate was able to prevent pitting of the passivated surface [34]. Although reduction of nitrate by Fe(II) is thermodynamically feasible, this reduction may not occur completely in the presence of the chloride ions[42].In this study sodium nitrate was used in the alkaline pore solution with high concentration of chloride ion (C_{cirt}), which probably cannot form a dominant phase of iron nitrate ($Fe[NO_3]_2$) to form a passive film.

The inhibition efficiency of 11AD is significantly higher than that of sodium nitrate which may be related to the partial absorption of this inhibitor on the surface of the reinforcing steel. This behaviour is relate to the formation of chemical bonds with reinforcing steel[43]. 4-AB did not show sufficient IE in pore solution but changed the corroding potential (-0.52 V) to the more noble value of -0.360 V. The corrosion current density in presence of 4-AB was higher than the samples without inhibitors (Table 4 and Figure 4). The amino group in 4-AB is responsible for surface adsorption and it is widely used to form an amino cation radical and subsequent chemical bonding of the radicals to the surface [44]. However, studies show that amino cations only form at high potential of oxidation (at~0.9 V) [45] and therefore the hindering the anodic reaction on the reinforcing steel can be related to the dissociation of carboxylate groups in 4-AB.The main advantage of 4-AB is that this inhibitor hindered anodic reaction significantly and delayed pitting potential to the value of E=0.640V due to presence of carboxylate groups . However, this inhibitor could not form a durable passive layer with constant current density on the reinforcing steel which may be linked to the weak absorption on the surface and lack of amino cations adsorption. In addition, 4AB promotes oxygen reaction in the cathodic sites which was indicated with a high value of b_c=301.

Table 4: Influence of corrosion inhibitors in current density, corrosion potential and %IE performance when [Cl]/[OH]=2

Inhibitor	b_c (V/decade)	b_a (V/decade)	B (V)	E_{corr} (V)	i_{corr} (μA/cm^2)	%IE
Control (no inhibitor)	0.141	0.089	0.023	-0.52	4.90×10^{-7}	N.D
Casein	0.124	0.284	0.037	-0.37	9.19×10^{-8}	82
11-AD	0.120	0.170	0.029	-0.54	2.38×10^{-7}	52
4 -ABA	0.301	0.662	0.089	-0.36	2.31×10^{-6}	Negative effect
sodium nitrate	0.167	116	0.029	-0.51	4.23×10^{-7}	14

The electrochemical behaviour of the reinforcing steel in the presence of casein was illustrated in Figure 4. The casein provided the passive film in the broad range of potential during anodic scan and the pitting potential reached the value of E_{pit} = 0.620V. In addition, corrosion potential shifted to the positive potential, -0.380V, and a passive film with the constant current density was observed. Casein exhibits an amphiprotic structure due to the NH_2 and COOH functions, so it can be dissolved in high pH solution [46]. The potential shift can be related to the formation a carboxylate bond between the casein and the reinforcing steel which consequently blocks anodic reaction of the reinforcing steel[20,46,47]. The changes in the Tafel slope with inhibitors are mostly attributed to a change in the rate determining step or the influence of adsorbed inhibitor in intermediate reactions [48]. The anodic Tafel slopes (ba) with addition of various inhibitors represented in Table 4 and this table shows that corrosion inhibitors increased the anodic Tafel slope (ba) which can be related to the adsorption of inhibitors onto the metal surface and subsequently hindered the passage of metallic ions into the solution and blocking

reaction sites therefore affecting the anodic reaction mechanism. Casein with the ba=0.284 and 4AB with the ba=0.662 represented the highest adsorption capacity but the cathodic Tafel slope (bc) of the 4AB was significantly different from other inhibitors and negatively facilitated the cathodic reactions on the surface of the reinforcing steel which subsequently changed the mechanism of inhibition of this inhibitor . The oxygen reduction on the surface of the refining steel possibly removed the adsorbed 4-AB from the surface and decreased the inhibition performance. The IE of the casein was higher than the other inhibitors which may related to presence of carboxylate functional groups in casein molecular structure. The polarity of this functional group promotes adsorption of casein through the negative charge localisation on oxygen and develops a repulsive action towards chloride ions, which restricts chloride activities on the reinforcing steel [49].

2.3 Electrochemical impedance spectroscopy

The Nyquist plot for reinforcing steel in the presence of various types of corrosion inhibitors is shown in Figure 5. The radius of capacitive loops in the low frequency in presence of casein and 11AB is higher than other inhibitors. Particularly, the Nyquist plot of casein shows the larger capacitive loop in comparison with 11AB which suggests the highest corrosion resistance is obtained in the presence of casein. In addition, a zoomed Nyquist plot at full impedance range shows the performance of nitrate and 4-AB in corrosion protection for reinforcing steel at Cl/OH=2 although it is not significant.

The Bode plot of the reinforcing steel in the pore solution with and without inhibitors in the presence of C_{cirt} is shown in Figure 5.

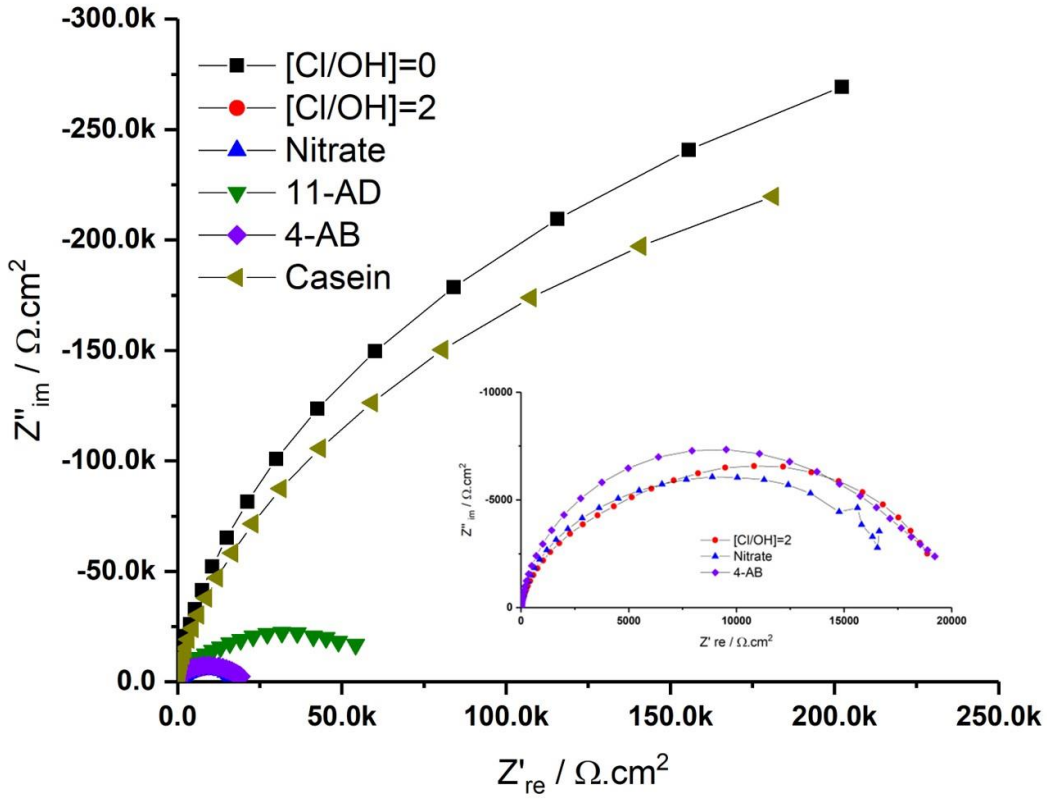

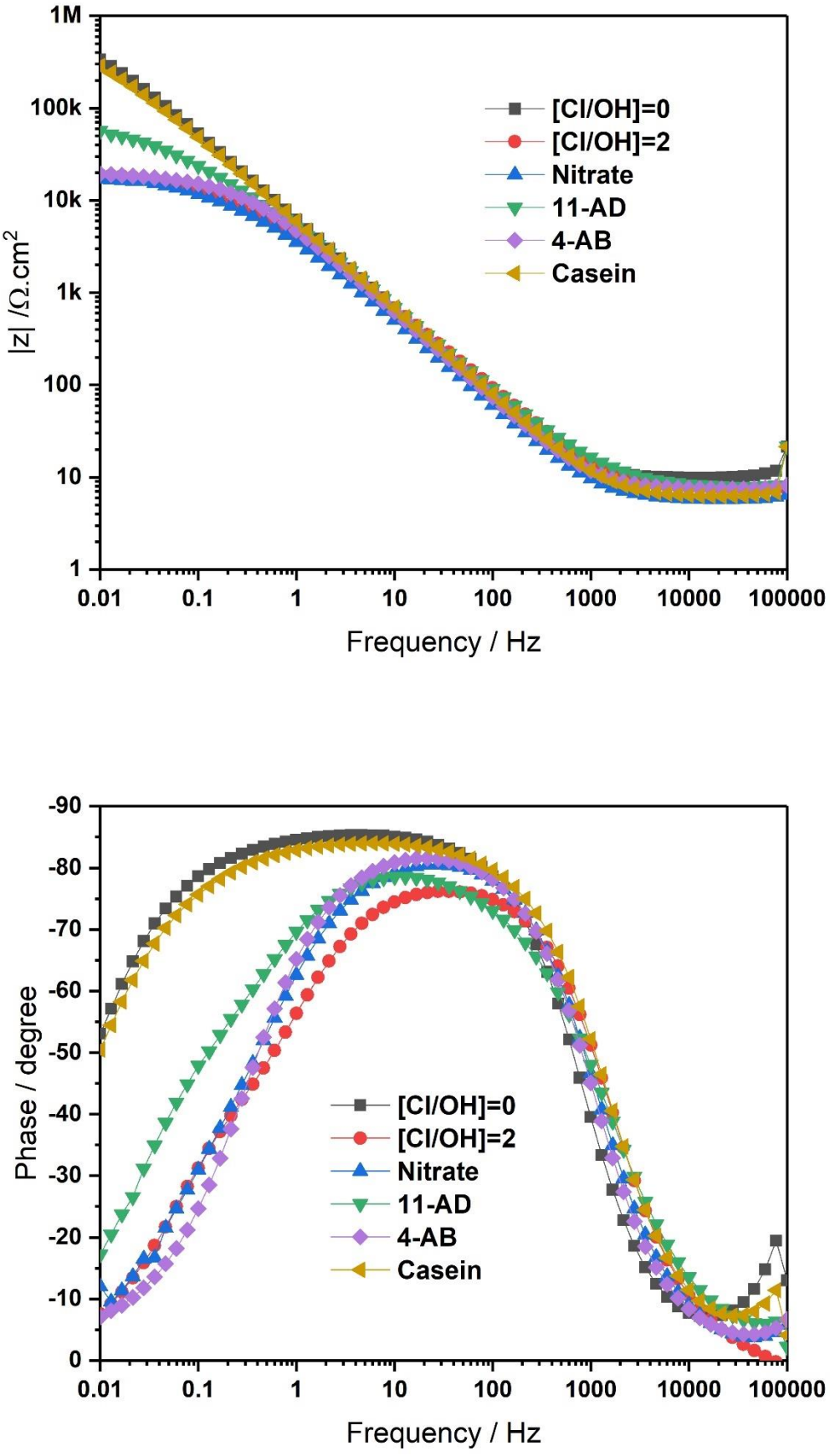

Figure 5: Nyquist and Bode plot of the reinforcing steel exposed to the various corrosion inhibitors containing critical concentration of chloride in the solution

The performance of inhibitors can be evaluated with the analysis of the Bode plot at low frequency, since the low frequency of impedance is attributed to the interaction of metals with the surrounding environment. The inhibitors in the pore solution can interact with the reinforcing steel and hinder oxidation and reduction reactions. The impedance modulus of the reinforcing steel in the pore solution, after 24 hours of immersion, with the C_{crit} reached the value of 20 kΩ.cm^2. This value is much lower than 300 kΩ.cm^2 measured without C_{crit} and this clearly indicated the effect of chloride ions in the corrosion activity of the reinforcing steel.

The value of the impedance modulus with the application of sodium nitrate (0.05M) and 4AB (0.05M) did not show a significant change in the low frequency range. This can be attributed to the weak absorption of these inhibitors on the reinforcing steel. The same concentration of 11AD (0.5M) increased the modulus of impedance to the value of 60kΩ.cm2, which represents the protection of reinforcing steel in the pore solution. However, higher corrosion protection was achieved by using Casein (9.7×10^{-4}M), which significantly increased the modulus of impedance to the value of 290 kΩ.cm^2. This value is 14 times higher than the pore solution containing C_{crit} and it shows that the casein hindered oxidation and reduction processes significantly. In addition, casein provides repulsive action against chloride ions and subsequently the access of chloride ions to the reinforcing steel becomes limited[50]. The Modulus value of the reinforcing steel in the pore solution without chloride ions showed a similar modulus value, 300 kΩ.cm2, indicating the effectiveness of this corrosion inhibitor.

The behaviour of reinforcing steel in pore solution at high frequency (10^3-10^5) with and without inhibitors does not exhibit specific changes in phase angle but the effect of inhibitors is clearly detectable at the low frequency domain (0.01-10^3). The phase angle of the reinforcing steel in the pore solution without inhibitor developed a broad time constant which decreased to a narrow one in presence of the chloride ions (C_{crit}). The inhibitors at low frequency changed the width of the time constant and allowed the evaluation of the performance of the inhibitors. Sodium nitrates shifted the time constant to the more negative angles at middle frequencies (1-100) indicating enhanced capacitive properties. However, this behaviour did not continue at lower frequencies and followed the behaviour of the corroding steel. 4AB at low frequency (<1Hz) showed a low phase angle, which was worse than corroding steel in C_{cirt}. 11AD and casein provided a wider time constant and higher phase angle in comparison to the other inhibitors indicating an enhanced corrosion protection.

the specific corrosion parameters were determined using appropriate equivalent circuits which have been developed and reported for reinforcing steel in alkaline solutions (Figure 6)[51–53]. The impedance data was fitted to the proposed equivalent circuit (EC) by using Zview software. Each element in this equivalent circuit represents the physical phenomenon or an electrochemical reaction occurring at the electrode. Rs in the proposed model denotes the resistance of the electrolyte solution. Rct as a charge transfer resistance element represents the difficulty of electron transfer between the the anodic dissolution and reduction processes. constant phase elements (CPEs) in these models defined as $Z = 1/[Y (j*\omega)n]$ where Y is the basic admittance, ω is the angular frequency equal to 2πf and n is a constant which can be changed due to the heterogeneity of the surface. The value of n=1 changes the constant phase element to the pure capacitor, Resistance at n=0 and inductance at n=-1[54]. However, when the value of n=0.5, constant phase element represents Warburg impedance in which the mass transport is a dominant process. The dispersion from the pure capacitor(n=1) is explained by formation of the rough surface due to the adsorption of inhibitors, dislocation or formation of a porous layer[55].

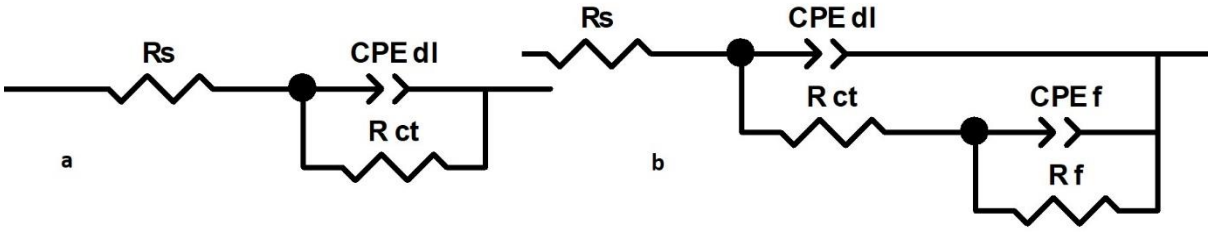

Figure 6: Equivalent circuit used to model the impedance data a) used for reinforcing steel in pore solution without chloride ions b) used for reinforcing steel in pore solution with C_{crit}, 4-AB and 11-AD and casein

Two ECs were proposed for the analysis of the electrochemical behaviour in the pore solution. Figure 6a was used for spectra fitting of the reinforcing steel in the pore solution without chloride ions. The second model (Figure 6b) was used for modelling the electrochemical behaviour of the reinforcing steel in the pore solution containing the other inhibitors.
CPE_{dl} can also represent the effect of inhibitors on the surface of the reinforcing steel. R_f and CPE_f represente the variation of the resistance and capacitance of the passive film in presence of chloride or corrosion inhibitors, respectively. Therefore, it was possible to distinguish the behaviour of the passive film and inhibitor. The fitting results of the impedance data were shown in Table 5.

Table 5: Fitted data of the equivalent circuit parameters for the reinforcing steel exposed to different solutions

Reinforcing steel	**Rs/Ω cm2**	**CPE_{dl} $Y0/\Omega^{-1}cm^{-2}$ s^n**	**n**	**Rct/Ω cm2**	**Rf/Ω cm^2**	**CPE_f $Y0/\Omega^{-1}cm^{-2}$ s^n**	**n**	**Chi-Sqr**
Pore solution	10	2.95×10^{-5}	0.95	561k	---	----	---	0.008
Pore solution +C_{crit}	10	3.57×10^{-5}	0.89	7921	12385	0.0001008	0.74	0.0003
Pore solution +C_{crit}+casein	10	3.69×10^{-5}	0.93	331k	127k	0.0000803	0.81	0.009
Pore solution +C_{crit}+nitrate	10	4.22×10^{-5}	0.93	7630	11440	0.00011109	0.71	0.001
Pore solution +C_{crit}+4-AB	10	3.89×10^{-5}	0.94	9725	13037	0.0000129	0.70	0.001
Pore solution +C_{crit}+11-AD	10	3.72×10^{-5}	0.89	25015	36853	6.92E-05	0.79	0.001

The results suggested that critical concentration of chloride ions played an important role in modelling of the impedance data. R_{ct} was higher than 650 kΩ cm^2 in pore solution without chloride ions but it dramatically dropped to the value of 7.9 kΩ cm^2 at critical concentration of chloride ions .The concentration of OH^- in pore solution was associated with the value of double layer capacitance. The corrosion initiation of the reinforcing steel generally is related to the decreasing of pH in solution or OH concentration, described earlier in section 2.1.1. The decrease of the OH at the interface was linked to the increasing of the double layer capacitance. Although it was possible to detect the decrease of OH at the interface with electrochemical modelling, the PH-meter did not show significant changes in the pH of the pore solution (results not shown here). It is because the concentration of the OH was changed locally and only at the interface. The chloride ions decreased the charge transfer resistance due to the decrease of OH and subsequently developed a new time constant denoted as Rf and CPE_f in the model. The value of n which represents the inhomogeneity of the double layer capacitance decreased to 0.89 indicating the effect of OH concentration in increasing the inhomogeneity of the CPEdl. This behaviour in turn increased CPE_{dl} to the value of 3.57×10^{-5} $Y0/\Omega^{-1}cm^{-2}$ s^n in comparison to the reinforcing steel in pore solution. In addition, formation of a new time constant at low frequency with the n=0.74 can be related to the formation of the porous layer within the passive film at critical level of chloride concentration. This behaviour is related to the attacks of the chloride ions on the passive layer of reinforcing steel and represent of inhomogeneity in the surface[56].

It was possible to evaluate the behaviour of the inhibitors with monitoring the variation of the R_f in pore solution and it was found that sodium nitrate and 4-AB did not show significant changes in passive film resistance and the n value of CFE_f were 0.71 and 0.70 respectively. This behaviour shows the adsorption of this inhibits to the passive layer is not significant which is in agreement with our finding in the potentiodyamic polarisation test. However, in the case of 11-AD the value of R_f increased four times

in comparison to the system without inhibitors and reached the value of 36 kΩ cm^2 and this value is significantly higher than R_f in 4AB and sodium nitrate.

The R_f in case of casein showed a significant increase and reached the value of 127 kΩ cm^2 which was a much higher value than other inhibitors. The constant phase element CFE_f which was assigned for passive film in the presence of casein decreased to the value of 8.03×10^{-5} $Y0/\Omega^{-1}cm^{-2}$ s^n. this decrease can be related to the adsorption of casein into the interface or substitution of water molecule with casein. The capacitance value of the passive film can be calculated from the CPE parameters according to the following equation(Equation 5)[57].

$$C = \frac{Y\,\omega^{n-1}}{\sin(n(\frac{\pi}{2}))} \qquad \text{Equation (5)}$$

And according to the Helmholtz model (Equation 6)the value of the capacitor depends on the surface area of the working electrode (A) and thickness of the passive film(d) and local dielectric constant(ε) and permittivity(ε_0) [57].

$$C = \frac{A\varepsilon\varepsilon_0}{d} \qquad \text{Equation (6)}$$

Therefore, decrease in CPE is related to either the thickening of the passive film or decreasing the dielectric constant due to the adsorption of casein to the surface. The inhibition mechanism of casein as explained earlier, is not only based on adsorption of casein to the reinforcing steel but also providing repulsive action against chloride ions. The chloride ions attack to the passive film was restricted significantly which can be seen in R_f. The CPE_{dl} value for casein is 3.69×10^{-5} $Y0/\Omega^{-1}cm^{-2}$ s^n, which is close to the value of the other inhibitors and it is higher than the reference sample indicating lower OH^- concentration on the interface due to the presence of inhibitors.

Conclusion

Corrosion behaviour of reinforcing steel in various concentrations of chloride solution was studied and the critical chloride concentration for corrosion initiation was determined. In addition, the performance of four types of environmentally friendly inhibitors in this critical chloride concentration were evaluated and the following conclusions are drawn.

1- The open circuit potential (OCP) of the reinforcing steel shows a clear relation to the chloride concentration of the synthetic pore solution. Increasing chloride concentration shifts the potential to the more cathodic value. The first radical change of potential due to the increasing of chloride concentration demonstrates the chloride threshold value and subsequent corrosion initiation. In addition, OCP can be considered as a criterion for evaluating the efficiency of the inhibitors in a pore solution containing C_{crir}. The more effective inhibitors shift the OCP to the nobler potential.

2- De-passivation of the reinforcing steel was accrued at [Cl]/[OH]=2 and most likely, was associated with a drop in polarisation resistance (Rp)

3- The Potentiodyamic polarisation curves of the four types of inhibitors used in this research indicated a considerable decrease in corrosion current density and noticeable increase in pitting potential in the presence of casein and 11-AD respectively. Sodium nitrate and 4-AB represented insufficient protection in C_{crit} but 4-AB decreased the rate of anodic reaction without forming a passive film.

4- The appropriate equivalent circuit with two time constants was considered to interpret and model the impedance data in presence of corrosion inhibitors. This model allowed extracting various parameters that contribute to the performance of corrosion inhibitors. The influence of corrosion inhibitors was significant in R_f in the proposed model. The efficiency of corrosion inhibitors changed with the following rank: casein >11-AD > 4-AB > sodium nitrate. It was confirmed that casein as a green corrosion inhibitor significantly enhance the corrosion protection of reinforcing steel at pore solution containing C_{crir}.

5. Casein as a green corrosion inhibitor provides a sufficient corrosion protection to the reinforcing steel and it can be used instead of toxic corrosion inhibitors. However, further experiments are necessary to evaluate its influence in concrete and different environments over time.

Acknowledgments

The authors gratefully acknowledge Engineering and Physical Science Research Council (EPSRC) for funding Resilient Materials 4 Life (RM4L) under EP/P02081X/1 project.

References

[1] A. Kenny, A. Katz, Steel-concrete interface influence on chloride threshold for corrosion – Empirical reinforcement to theory, Constr. Build. Mater. 244 (2020) 118376. https://doi.org/10.1016/j.conbuildmat.2020.118376.

[2] G. Koch, Cost of corrosion, Elsevier Ltd, 2017. https://doi.org/10.1016/B978-0-08-101105-8.00001-2.

[3] M.G. Sohail, R. Kahraman, N.A. Alnuaimi, B. Gencturk, W. Alnahhal, M. Dawood, A. Belarbi, Electrochemical behavior of mild and corrosion resistant concrete reinforcing steels, Constr. Build. Mater. (2020). https://doi.org/10.1016/j.conbuildmat.2019.117205.

[4] J.K. Das, B. Pradhan, Effect of cation type of chloride salts on corrosion behaviour of steel in concrete powder electrolyte solution in the presence of corrosion inhibitors, Constr. Build. Mater. 208 (2019) 175–191. https://doi.org/10.1016/j.conbuildmat.2019.02.153.

[5] J. Chen, C. Fu, H. Ye, X. Jin, Corrosion of steel embedded in mortar and concrete under different electrolytic accelerated corrosion methods, Constr. Build. Mater. 241 (2020) 117971. https://doi.org/10.1016/j.conbuildmat.2019.117971.

[6] B. Beverskog, I. Puigdomenech, Revised Pourbaix diagrams for iron at 25-300°C, Corros. Sci. (1996). https://doi.org/10.1016/S0010-938X(96)00067-4.

[7] A. James, E. Bazarchi, A.A. Chiniforush, P. Panjebashi Aghdam, M.R. Hosseini, A. Akbarnezhad, I. Martek, F. Ghodoosi, Rebar corrosion detection, protection, and rehabilitation of reinforced concrete structures in coastal environments: A review, Constr. Build. Mater. 224 (2019) 1026–1039. https://doi.org/10.1016/j.conbuildmat.2019.07.250.

[8] R.K.L. Su, Y. Zhang, A novel elastic-body-rotation model for concrete cover spalling caused by non-uniform corrosion of reinforcement, Constr. Build. Mater. 213 (2019) 549–560. https://doi.org/10.1016/j.conbuildmat.2019.04.096.

[9] M. Babaee, A. Castel, Chloride diffusivity, chloride threshold, and corrosion initiation in reinforced alkali-activated mortars: Role of calcium, alkali, and silicate content, Cem. Concr. Res. 111 (2018) 56–71. https://doi.org/10.1016/j.cemconres.2018.06.009.

[10] U. Angst, B. Elsener, C.K. Larsen, Ø. Vennesland, Critical chloride content in reinforced concrete - A review, Cem. Concr. Res. (2009). https://doi.org/10.1016/j.cemconres.2009.08.006.

[11] J. Zhang, J. Guo, D. Li, Y. Zhang, F. Bian, Z. Fang, The influence of admixture on chloride time-varying diffusivity and microstructure of concrete by low-field NMR, Ocean Eng. 142 (2017) 94–101. https://doi.org/10.1016/j.oceaneng.2017.06.065.

[12] Y. Cao, C. Gehlen, U. Angst, L. Wang, Z. Wang, Y. Yao, Critical chloride content in reinforced concrete — An updated review considering Chinese experience, Cem. Concr. Res. (2019). https://doi.org/10.1016/j.cemconres.2018.11.020.

[13] T. Ishida, S. Miyahara, T. Maruya, Chloride binding capacity of mortars made with various portland cements and mineral admixtures, J. Adv. Concr. Technol. 6 (2008) 287–301. https://doi.org/10.3151/jact.6.287.

[14] A.S. Fazayel, M. Khorasani, A.A. Sarabi, The effect of functionalized polycarboxylate structures as corrosion inhibitors in a simulated concrete pore solution, Appl. Surf. Sci. 441 (2018) 895–913. https://doi.org/10.1016/j.apsusc.2018.02.012.

[15] V. Shubina Helbert, L. Gaillet, T. Chaussadent, V. Gaudefroy, J. Creus, Rhamnolipids as an eco-friendly corrosion inhibitor of rebars in simulated concrete pore solution: evaluation of conditioning and addition methods, Corros. Eng. Sci. Technol. 55 (2020) 91–102. https://doi.org/10.1080/1478422X.2019.1672008.

[16] C. Sun, M. Chen, H. Zheng, P. Zhang, Y. Li, B. Hou, The effect of amino-alcohol-based corrosion inhibitors on concrete durability, Can. J. Civ. Eng. 46 (2019) 771–776. https://doi.org/10.1139/cjce-2018-0482.

[17] N. Gartner, T. Kosec, A. Legat, The efficiency of a corrosion inhibitor on steel in a simulated concrete environment, Mater. Chem. Phys. (2016). https://doi.org/10.1016/j.matchemphys.2016.08.047.

[18] M.. Paridah, A. Moradbak, A.. Mohamed, F. abdulwahab taiwo Owolabi, M. Asniza, S.H.. Abdul Khalid, We are IntechOpen , the world ' s leading publisher of Open Access books Built by scientists , for scientists TOP 1 %, Intech. i (2016) 13. https://doi.org/http://dx.doi.org/10.5772/57353.

[19] C. Pan, X. Li, J. Mao, The effect of a corrosion inhibitor on the rehabilitation of reinforced concrete containing sea sand and seawater, Materials (Basel). 13 (2020). https://doi.org/10.3390/ma13061480.

[20] N.P. Cosman, K. Fatih, S.G. Roscoe, Electrochemical impedance spectroscopy study of the adsorption behaviour of α-lactalbumin and β-casein at stainless steel, J. Electroanal. Chem. 574 (2005) 261–271. https://doi.org/10.1016/j.jelechem.2004.08.007.

[21] G.Daufin. Jean-Luc AUDICa, Bernard CHAUFER, A, Non-food applications of milk components and dairy co-products: A review, J. Food Prot. 72 (2009) 2162–2169. https://doi.org/10.1051/lait.

[22] H. Bian, J. Plank, Surface phenomena related to applications regarding optimum dosages of casein superplasticizer in self-leveling underlayment cements, Zeitschrift Fur Naturforsch. - Sect. B J. Chem. Sci. 74 (2019) 607–611. https://doi.org/10.1515/znb-2019-0092.

[23] A. Poursaee, Corrosion of steel bars in saturated Ca(OH)2 and concrete pore solution, Concr. Res. Lett. 1 (2010) 90–97. http://www.issres.net/journal/index.php/crl/article/view/106.

[24] R.S. Resender, NACE corrosion engineer's reference book., (1980) 88.

[25] M. Kouřil, P. Novák, M. Bojko, Limitations of the linear polarization method to determine stainless steel corrosion rate in concrete environment, Cem. Concr. Compos. 28 (2006) 220–225. https://doi.org/10.1016/j.cemconcomp.2006.01.007.

[26] L. Freire, X.R. Nóvoa, M.F. Montemor, M.J. Carmezim, Study of passive films formed on mild steel in alkaline media by the application of anodic potentials, Mater. Chem. Phys. 114 (2009) 962–972. https://doi.org/10.1016/j.matchemphys.2008.11.012.

[27] J. Williamson, O.B. Isgor, The effect of simulated concrete pore solution composition and chlorides on the electronic properties of passive films on carbon steel rebar, Corros. Sci. 106 (2016) 82–95. https://doi.org/10.1016/j.corsci.2016.01.027.

[28] E. Volpi, A. Olietti, M. Stefanoni, S.P. Trasatti, Electrochemical characterization of mild steel in alkaline solutions simulating concrete environment, J. Electroanal. Chem. 736 (2015) 38–46. https://doi.org/10.1016/j.jelechem.2014.10.023.

[29] M.F. Montemor, A.M.P. Simões, M.G.S. Ferreira, Chloride-induced corrosion on reinforcing steel: From the fundamentals to the monitoring techniques, Cem. Concr. Compos. 25 (2003)

491–502. https://doi.org/10.1016/S0958-9465(02)00089-6.

[30] P. Ghods, O.B. Isgor, G.A. McRae, G.P. Gu, Electrochemical investigation of chloride-induced depassivation of black steel rebar under simulated service conditions, Corros. Sci. (2010). https://doi.org/10.1016/j.corsci.2010.02.016.

[31] H. DorMohammadi, Q. Pang, P. Murkute, L. Árnadóttir, O.B. Isgor, Investigation of chloride-induced depassivation of iron in alkaline media by reactive force field molecular dynamics, Npj Mater. Degrad. 3 (2019). https://doi.org/10.1038/s41529-019-0081-6.

[32] C. Test-, StandardTest Method for Corrosion Potentials of Uncoated Reinforcing Steel in, (2020) 1–7. https://doi.org/10.1520/C0876-09.2.

[33] J. Gui, T.M. Devine, A SERS investigation of the passive films formed on iron in mildly alkaline solutions of carbonate/bicarbonate and nitrate, Corros. Sci. 37 (1995) 1177–1189. https://doi.org/10.1016/0010-938X(94)00179-A.

[34] H.Y. Ma, C. Yang, G.Y. Li, W.J. Guo, S.H. Chen, J.L. Luo, Influence of nitrate and chloride ions on the corrosion of iron, Corrosion. 59 (2003) 1112–1119. https://doi.org/10.5006/1.3277530.

[35] Y. Nie, J. Gao, E. Wang, L. Jiang, L. An, X. Wang, An effective hybrid organic/inorganic inhibitor for alkaline aluminum-air fuel cells, Electrochim. Acta. 248 (2017) 478–485. https://doi.org/10.1016/j.electacta.2017.07.108.

[36] S. Rengaraju, L. Neelakantan, R.G. Pillai, Investigation on the polarization resistance of steel embedded in highly resistive cementitious systems – An attempt and challenges, Electrochim. Acta. 308 (2019) 131–141. https://doi.org/10.1016/j.electacta.2019.03.200.

[37] M. Babaee, A. Castel, Chloride-induced corrosion of reinforcement in low-calcium fly ash-based geopolymer concrete, Cem. Concr. Res. 88 (2016) 96–107. https://doi.org/10.1016/j.cemconres.2016.05.012.

[38] Z. Wu, H. Yu, H. Ma, J. Zhang, B. Da, H. Zhu, Rebar corrosion in coral aggregate concrete: Determination of chloride threshold by LPR, Corros. Sci. 163 (2020). https://doi.org/10.1016/j.corsci.2019.108238.

[39] C. Alonso, C. Andrade, M. Izquierdo, X.R. Nóvoa, M.C. Pérez, Effect of protective oxide scales in the macrogalvanic behaviour of concrete reinforcements, Corros. Sci. 40 (1998) 1379–1389. https://doi.org/10.1016/S0010-938X(98)00040-7.

[40] M. Liu, X. Cheng, X. Li, C. Zhou, H. Tan, Effect of carbonation on the electrochemical behavior of corrosion resistance low alloy steel rebars in cement extract solution, Constr. Build. Mater. (2017). https://doi.org/10.1016/j.conbuildmat.2016.10.003.

[41] J.G.N. Thomas, T.J. Nurse, The anodic passivation of iron in solutions of inhibitive anions, Br. Corros. J. 2 (1967) 13–20. https://doi.org/10.1179/000705967798327208.

[42] C.J. Ottley, W. Davison, W.M. Edmunds, Chemical catalysis of nitrate reduction by iron(II), Geochim. Cosmochim. Acta. 61 (1997) 1819–1828. https://doi.org/10.1016/S0016-7037(97)00058-6.

[43] S. Ghareba, S. Kwan, S. Omanovic, Inhibition of carbon steel corrosion by 11-aminoundecanoic acid, J. Electrochem. Sci. Eng. 5 (2015) 157–172. https://doi.org/10.5599/jese.242.

[44] G. Yang, Y. Shen, M. Wang, H. Chen, B. Liu, S. Dong, Copper hexacyanoferrate multilayer films on glassy carbon electrode modified with 4-aminobenzoic acid in aqueous solution, Talanta. 68 (2006) 741–747. https://doi.org/10.1016/j.talanta.2005.05.017.

[45] L. Adamczyk, A. Pietrusiak, H. Bala, Corrosion resistance of stainless steel covered by 4-aminobenzoic acid films, Cent. Eur. J. Chem. 10 (2012) 1657–1668. https://doi.org/10.2478/s11532-012-0082-6.

[46] F. Berrekhis, Y. Roques, L. Aries, M. Hajjaji, Electrodeposition and characterization of casein

coatings on a zinc alloy, Prog. Org. Coatings. 33 (1998) 7–13. https://doi.org/10.1016/S0300-9440(97)00113-6.

[47] A. Yabuki, M. Sakai, Self-healing coatings of inorganic particles using a pH-sensitive organic agent, Corros. Sci. 53 (2011) 829–833. https://doi.org/10.1016/j.corsci.2010.11.021.

[48] R.T. Loto, C.A. Loto, T. Fedotova, Electrochemical studies of mild steel corrosion inhibition in sulfuric acid chloride by aniline, Res. Chem. Intermed. 40 (2014) 1501–1516. https://doi.org/10.1007/s11164-013-1055-x.

[49] M. Ormellese, L. Lazzari, S. Goidanich, G. Fumagalli, A. Brenna, A study of organic substances as inhibitors for chloride-induced corrosion in concrete, Corros. Sci. 51 (2009) 2959–2968. https://doi.org/10.1016/j.corsci.2009.08.018.

[50] T. Rabizadeh, S.K. Asl, Casein as a natural protein to inhibit the corrosion of mild steel in HCl solution, J. Mol. Liq. 276 (2019) 694–704. https://doi.org/10.1016/j.molliq.2018.11.162.

[51] Y. Zhao, T. Pan, X. Yu, D. Chen, Corrosion inhibition efficiency of triethanolammonium dodecylbenzene sulfonate on Q235 carbon steel in simulated concrete pore solution, Corros. Sci. 158 (2019) 108097. https://doi.org/10.1016/j.corsci.2019.108097.

[52] Y. Cubides, H. Castaneda, Corrosion protection mechanisms of carbon nanotube and zinc-rich epoxy primers on carbon steel in simulated concrete pore solutions in the presence of chloride ions, Corros. Sci. 109 (2016) 145–161. https://doi.org/10.1016/j.corsci.2016.03.023.

[53] F. Zhang, J. Pan, C. Lin, Localized corrosion behaviour of reinforcement steel in simulated concrete pore solution, Corros. Sci. 51 (2009) 2130–2138. https://doi.org/10.1016/j.corsci.2009.05.044.

[54] M.S. Hasanin, S.A. Al Kiey, Environmentally benign corrosion inhibitors based on cellulose niacin nano-composite for corrosion of copper in sodium chloride solutions, Int. J. Biol. Macromol. 161 (2020) 345–354. https://doi.org/10.1016/j.ijbiomac.2020.06.040.

[55] A. Popova, M. Christov, Evaluation of impedance measurements on mild steel corrosion in acid media in the presence of heterocyclic compounds, Corros. Sci. 48 (2006) 3208–3221. https://doi.org/10.1016/j.corsci.2005.11.001.

[56] M.E. Orazem, J.-B. Jorcin, N. Pébère, B. Tribollet, CPE analysis by local electrochemical impedance spectroscopy, Electrochim. Acta. 51 (2006) 1473–1479. https://doi.org/10.1016/j.electacta.2005.02.128.

[57] I. Ahamad, R. Prasad, M.A. Quraishi, Inhibition of mild steel corrosion in acid solution by Pheniramine drug: Experimental and theoretical study, Corros. Sci. 52 (2010) 3033–3041. https://doi.org/10.1016/j.corsci.2010.05.022.